CHINA FOUNDRY Research & Development
Vol. 22 No. 3 May 2025
www.springer.com/41230
https://doi.org/10.1007/s41230-025-4041-1

Effect of melt superheating on solidification microstructure and mechanical properties of K424 superalloy

Gao-yang Jing[1, 2], Ao-qi Li[1, 2], *Xun Sun[1, 2], Lei Jin[1, 2], Cheng Zhou[1, 2], Dong-ping Zhan[3], and Ji-hang Li[3]

1. Shenyang Research Institute of Foundry Co., Ltd. CAM, Shenyang 110022, China

2. State Key Laboratory of Advanced Casting Technologies, Shenyang 110022, China

3. School of Metallurgy, Northeastern University, Shenyang 110819, China

Abstract: The effect of melt superheating treatment on the solidification microstructure and mechanical properties of the γ' phase precipitation-strengthened K424 superalloy was investigated. Differential scanning calorimetry (DSC) experiments were conducted to explore the influence of melt treatment temperature on the undercooling of the superalloy. Additionally, pouring experiments were carried out to assess how alterations in both the temperature and duration of melt treatment impacted the grain size, secondary dendrite arm spacing (SDAS), elemental segregation, and mechanical properties of the alloy. Metallographic analysis, scanning electron microscopy, energy dispersive spectroscopy (EDS) and Thermo-Calc software were employed for microstructure characterization. The test specimens were subjected to tensile testing at room temperature and stress rupture testing at 975 °C under 196 MPa. The findings reveal that appropriate melt treatment conditions result in decreased grain size, refined SDAS, minimized elemental segregation, and significant improvements in mechanical properties. Specifically, the study demonstrates that a melt treatment at 1,650 °C for 5 min results in the smallest average grain size of 949 μm and the smallest SDAS of 25.38 μm. Furthermore, the room temperature tensile properties and creep resistance are notably affected by the melt treatment parameters. It is shown that specific melt treatment conditions, such as holding at 1,650 °C for 5 min, result in superior room temperature strength and extended stress rupture life of the K424 superalloy, while a balance between strength and stability is achieved at 1,600 °C with a holding time of 10 min. These findings offer guidance for optimizing the melt treatment parameters for the K424 superalloy, laying a foundation for further investigations.

Keywords: melt superheating; K424 superalloy; solidification microstructure; elemental segregation; mechanical properties

CLC numbers: TG146.1+5 **Document code:** A **Article ID:** 1672-6421(2025)03-252-11

1 Introduction

Nickel-based polycrystalline superalloys are utilized in the production of aero-engine turbine blades due to their substantial strength, excellent structural stability, superior heat resistance, and lower production costs [1-4]. However, technological advancements in the aerospace industry have led to continuous enhancements in the thrust-to-weight ratio and operating temperatures of combustion chambers, thereby imposing more stringent demands on the performance of high-temperature structural materials [5].

Heat treatment processes can be utilized to enhance the comprehensive mechanical properties of superalloys by refining the as-cast solidification structure, reducing segregation, promoting the precipitation of strengthening phases, and thus achieving a uniform distribution of solid solution strengthening elements and phases within the matrix [6]. Nevertheless, given that solidification fundamentally involves a liquid-solid phase transition, the impact of melt characteristics on the solidification structure of castings should not be ignored. Research results showed that the liquid metal consists of atomic clusters with a specific number of nearest neighbors, and these clusters exhibit a crystal-like structure, interspersed with free atoms and electrons [7]. The melt structures

*Xun Sun

Male, born in 1964, Ph. D., Research Fellow. His research interests mainly focus on investment casting of superalloys.

E-mail: sx@foundrynations.com

Received: 2024-03-06; Revised: 2024-07-16; Accepted: 2024-07-24

could be influenced by variations in melt temperature [8-10], and these structural changes are proved through alterations in the physical parameters of melt [11, 12]. The melt structure, which is modified by melt superheating treatment, positively influences the subsequently formed solidification microstructure, thereby enhancing the comprehensive mechanical properties of alloy. Kolotukhin et al. [13] and Tyagunov et al. [14] have demonstrated that the melt structure undergoes alterations with an increase in temperature, which can effectively refine the microstructure and augment the mechanical properties of the superalloy. Jie et al. [15] investigated the solidification structure of IN718C superalloy across melt treatment temperatures ranging from 1,380 °C to 1,680 °C. The study revealed that higher melt treatment temperatures corresponded to a marked reduction in grain size and elemental segregation.

In summary, extensive research has been conducted to examine the impact of melt temperature on the melt structure, as well as the resulting alterations in microstructure and mechanical properties of alloys after solidification. However, the influence of melt treatment duration, a factor of equal significance, has not been sufficiently explored. This study focuses on the widely used material for high-pressure turbine blades, i.e., the γ' phase precipitation-strengthened K424 superalloy [16]. The influence of melt treatment temperature on the undercooling of this superalloy was studied through DSC experiments. On this basis, the effects of varying melt treatment temperatures and duration on grain size, secondary dendrite arm spacing (SDAS), elemental segregation, and mechanical properties were investigated by pouring experiments. The findings of this study assist in determining the optimal parameters for melt treatment of the K424 superalloy, thus providing a foundation for subsequent, more detailed research.

2 Materials and experiment

The material used in this study was the commercial K424 superalloy with a nominal chemical composition of Ni-9.6Cr-13.5Co-0.8Nb-8.9Mo-1.4W-4.45Ti-5.58Al-0.17C (percentage in weight). The DSC was employed to determine the characteristic temperature and other relevant information during the solidification process of K424 superalloy at varying melt superheating treatment conditions. The DSC test scheme is shown in Fig. 1.

A commercial alloy ingot weighing 5 kg was placed inside an alumina crucible within a ZGW25B vacuum induction melting furnace. The system was initially evacuated to a pressure of less than 0.1 Pa. After that, the power was increased until the desired melt treatment temperature (1,550 °C; 1,600 °C; 1,650 °C) was reached, which was then maintained for a specified period (5, 10, 20 min). It should be noted that pouring experiments at 1,650 °C were not carried out for durations of 10 min and 20 min due to two key factors: (1) longer exposure increases the reaction between the melt and the crucible, affecting the accuracy and reliability of results, and (2) extended high-temperature operation increases the risk of equipment damage. Following this, the temperature of the melt was rapidly lowered to 1,450 °C and held for 5 min. Finally, the melt was transferred into a corundum shell mould, preheated to 1,020 °C, within a span of 5 s. Table 1 lists the superheating treatment parameters for the melt. To standardize the cooling rate of the casting, the shell mould was embedded in sand, mitigating the impact of external environmental temperature fluctuations. Figure 2 presents the schematic illustration of the shell mould used in investment casting and the test specimen of K424 superalloy.

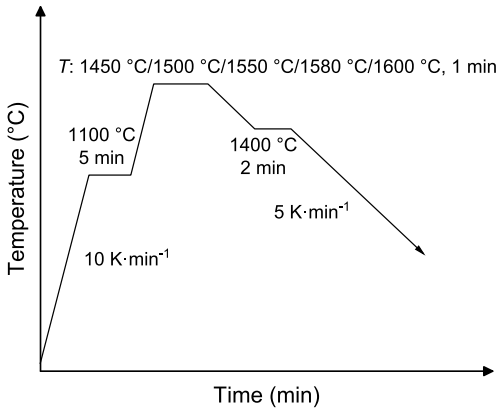

Fig. 1: DSC schematic diagram

Table 1: Parameters of melt superheating treatment

Superheating temperature (°C)	Duration (min)	Pouring temperature (°C)	Pouring time (s)
1,550	5	1,450	<5
	10		
	20		
1,600	5		
	10		
	20		
1,650	5		

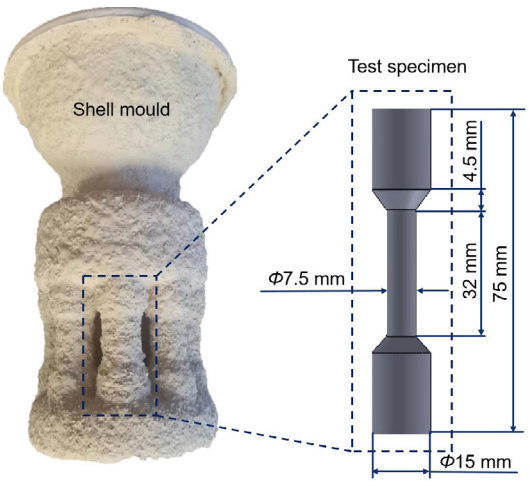

Fig. 2: Schematic diagram of the shell mould and test specimen

Following the sandblasting process to eliminate the residual shell mould on the casting surfaces, the test specimens were subsequently cut from the casting assembly. Tensile tests were conducted at room temperature, and stress rupture tests were performed at 975 °C and 196 MPa, in accordance with the Chinese National Military Standard GJB 5512.1-2005. Considering the variability in test outcomes, four test specimens were taken from each module. Of these, two were subjected to room temperature tensile testing, while the other two underwent stress rupture testing. The procedures for both room-temperature tensile testing and high-temperature creep testing followed the National Standards GB/T 228.1-2020 and GB/T 2039-2012, respectively.

The samples for metallographic analysis were sectioned transversely from the test specimens. Following grinding and polishing, samples were chemically etched with a solution composed of 1.5 g $CuSO_4$, 40 mL HCl, and 20 mL C_2H_5OH. A stereomicroscope, an optical microscope (OM, ZEISS Axio Vert. A1), and a scanning electron microscope (SEM, EVO MA25) were utilized to examine the solidification microstructures. The grain size on the cross-section was measured using standard quantitative metallographic techniques, and the SDAS was measured using the line intercept method. The SDAS (λ_2) was calculated using the equation: $\lambda_2=l/n$, where l is the length of the measured line, and n is the number of dendrite arms intersecting the line. At least five measurements were taken from different regions of each sample to ensure statistical reliability. The average SDAS and standard deviation were calculated. EDS was employed to semi-quantitatively analyze the chemical composition in the interdendritic regions and dendritic arms. For each area, at least three points of measurement were selected to ensure accuracy and reliability in the results.

3 Results

3.1 Microstructures of K424 superalloy

Figure 3 illustrates the microstructure of the K424 superalloy, which has been subjected to a melt treatment at 1,600 °C for 5 min. The element distribution within the microstructure of the alloy was analyzed utilizing the energy dispersive spectroscopy (EDS) mapping, and the results are shown in Fig. 4. It can be seen that the K424 superalloy primarily consists of the γ phase, γ' phase, a sunflower-like γ+γ' eutectic, and MC carbides. It should be noted that certain elements, including Ti, Nb, and Mo, that segregate significantly to the interdendritic region, are also major components of carbides. Conversly, it can be observed that Cr and Co are not the main components of the carbides. As shown in Fig. 4, the brightness of the area surrounding the interdendritic carbides is slightly higher than that of the dendritic arms, indicating that Cr and Co exhibit weak segregation in the interdendritic areas. To further clarify the composition of the solidified microstructure of the K424 superalloy, the Thermo-Calc software (Version 2019b) was utilized to calculate the fraction of the main phases at equilibrium conditions, as shown in Fig. 5. It is evident that the calculated results are essentially consistent with the experimental results except for the absence of σ phase and $M_{23}C_6$ carbides in the specimens, as well as the (γ+γ') eutectic structure in the calculated results. This discrepancy can be attributed to the difference between equilibrium cooling conditions and the actual cooling rate of the casting experiment, which varies the solidification process.

3.2 Grain size

Figure 6 illustrates average grain size of the as-cast solidification structure of K424 superalloy under various melt superheating conditions. The as-cast grains are predominantly equiaxed, but columnar grain structures are visible in the edge region of the samples after a treatment at 1,650 °C for a duration of 5 min. Moreover, the size of equiaxed grains in the central region at this treatment condition is smaller than

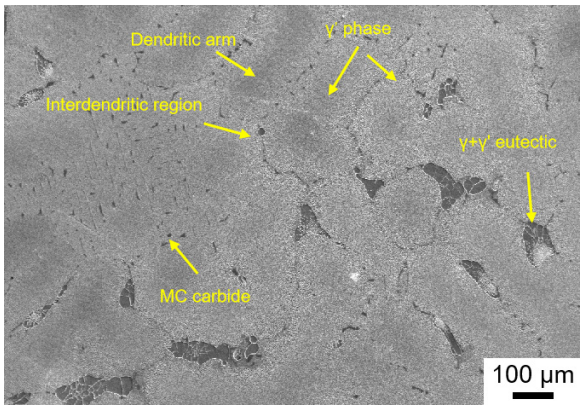

Fig. 3: SEM microstructure of the K424 superalloy

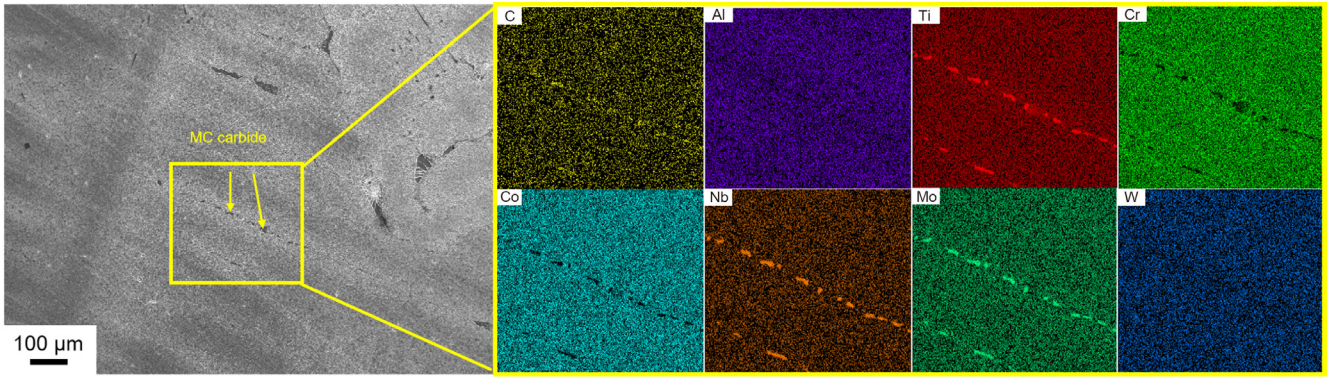

Fig. 4: EDS mapping results of as-cast microstructure of K424 superalloy

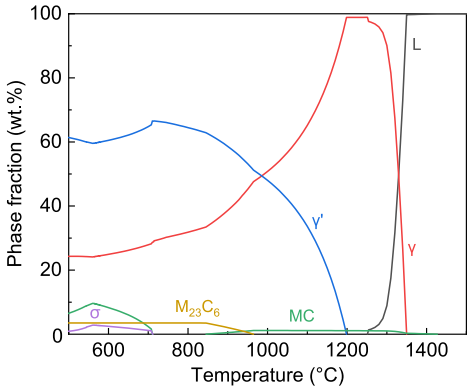

Fig. 5: Calculated fraction of phases as a function of temperature in K424 superalloy

their counterparts at other superheating conditions. The average grain size initially decreases and then increases with increased treatment time at a melt superheating condition of 1,550 °C. The size is 2,466 μm after holding for 5 min, reduces to 2,138 μm after 10 min, and finally increases to 2,590 μm after 20 min. At a superheating condition of 1,600 °C, the trend of grain size change is the same as that at 1,550 °C. The smallest average grain size of 1,582 μm is achieved after holding for 10 min. The average grain size, following a 5 min melt treatment, progressively decreases as the melt treatment temperature increases. The smallest average grain size of 949 μm is recorded at 1,650 °C for a duration of 5 min.

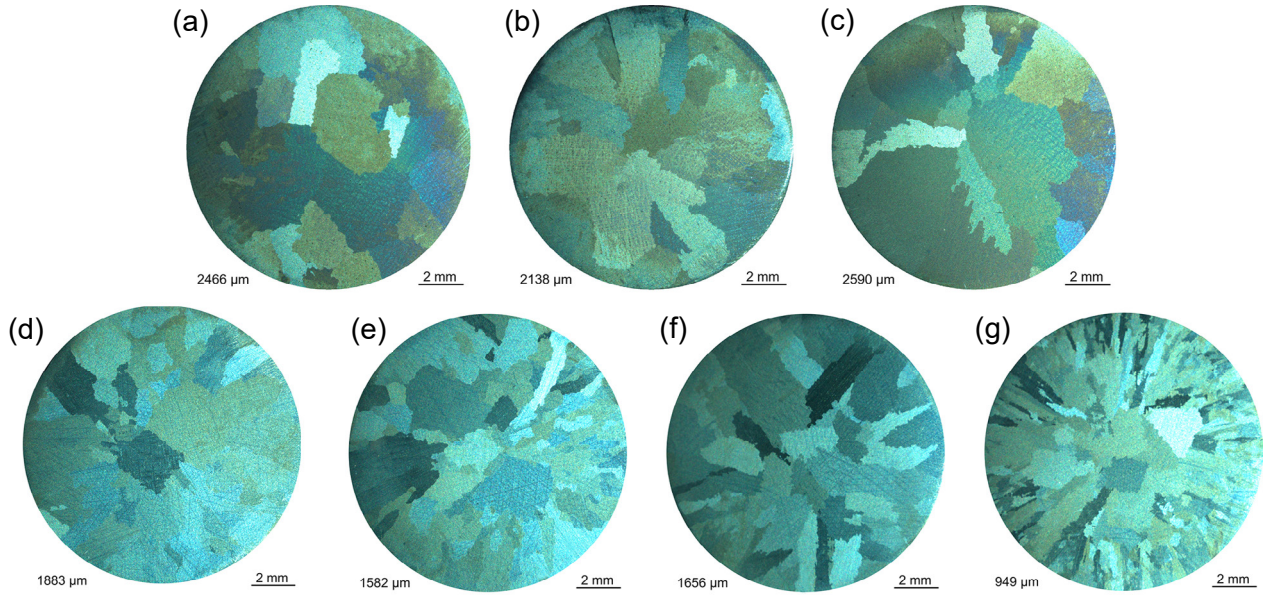

Fig. 6: Grain size of K424 superalloy superheated at different conditions; (a) 1,550 °C, 5 min; (b) 1,550 °C, 10 min; (c) 1,550 °C, 20 min; (d) 1,600 °C, 5 min; (e) 1,600 °C, 10 min; (f) 1,600 °C, 20 min; (g) 1,650 °C, 5 min

The experimental findings indicate that a suitable extension of the melt treatment duration, coupled with an elevation in treatment temperature, can result in a reduction in grain size. This, in turn, contributes to the enhancement of the comprehensive mechanical properties of the K424 equiaxed grain nickel-based cast superalloy.

3.3 Secondary dendritic arm spacing

Figures 7 and 8 illustrate the dendritic morphology and average SDAS of the K424 superalloy under various melt treatment conditions. In general, SDAS tends to decrease as the melt treatment temperature increases with the same treatment duration. At a treatment temperature of 1,550 °C, SDAS increases from 46.05 μm after a duration of 5 min to 52.44 μm after 10 min, but decreases to 41.78 μm after 20 min. At a treatment temperature of 1,600 °C, SDAS diminishes from 38.88 μm after a duration of 5 min to 31.76 μm after 10 min, and then ascends to 34.10 μm after 20 min. The minimum SDAS of 25.38 μm, is recorded at a superheating temperature of 1,650 °C for a duration of 5 min. These findings indicate that melt treatment temperature exerts a more pronounced influence on SDAS compared to treatment duration.

3.4 Element segregation

The redistribution of solute elements during solidification significantly influences the segregation behavior. The segregation coefficient k_i serves as a useful metric to quantify the degree of solute element segregation. In this research, the segregation coefficient k_i is defined as the element content ratio between the interdendritic region and dendritic arm.

Figure 9 shows the solute segregation coefficient of K424 superalloy at different melt superheating conditions. Figure 9 illustrates that the segregation coefficient k_i of Al and W elements is less than 1, suggesting these elements segregate to the dendritic arm. Conversely, the segregation coefficient k_i of Ti, Cr, Co, Nb, and Mo elements exceeds 1, signifying their segregation to the interdendritic region. Among all elements, Nb has the highest degree of segregation. As shown in Fig. 9(a), an increase in melt treatment temperature typically reduces the segregation degree of each element. However, the segregation

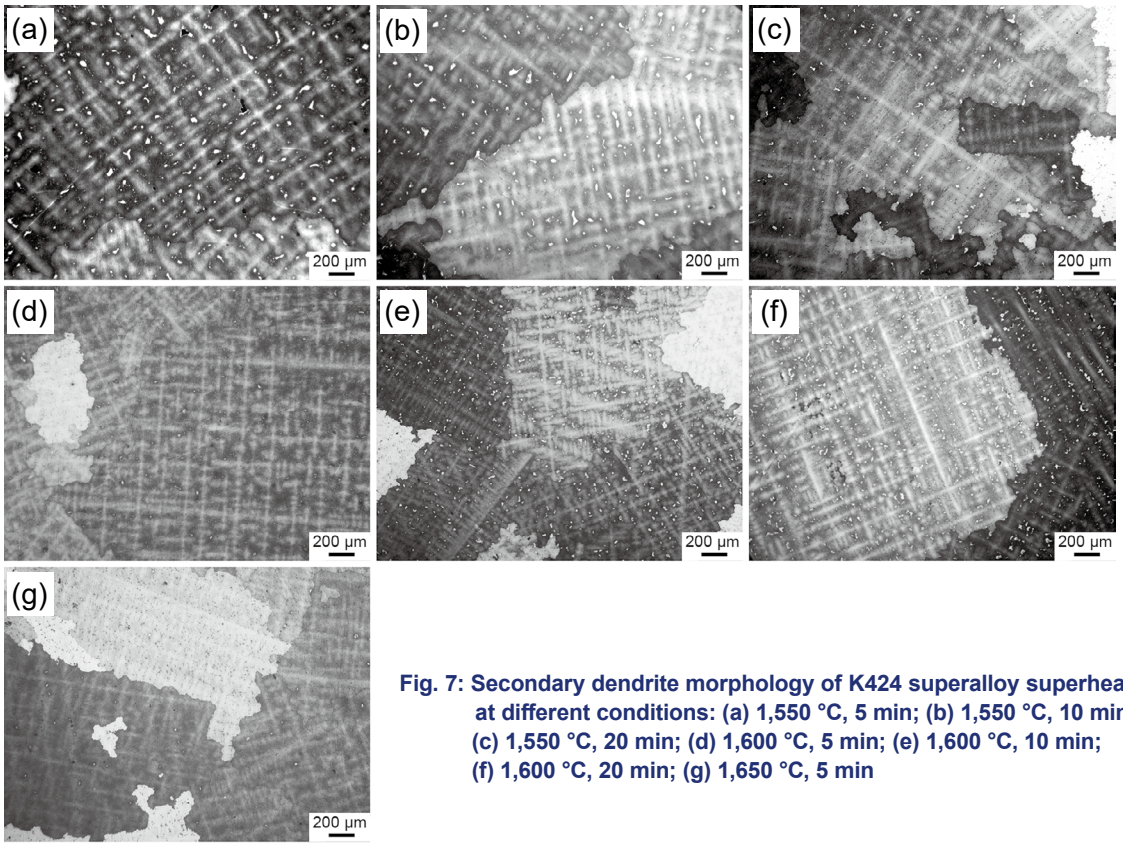

Fig. 7: Secondary dendrite morphology of K424 superalloy superheated at different conditions: (a) 1,550 °C, 5 min; (b) 1,550 °C, 10 min; (c) 1,550 °C, 20 min; (d) 1,600 °C, 5 min; (e) 1,600 °C, 10 min; (f) 1,600 °C, 20 min; (g) 1,650 °C, 5 min

coefficients of Al and Cr elements rise at 1,650 °C compared to 1,600 °C, which may be caused by changes in the melt structure due to the consumption of each melt elements at high superheating temperature. Figure 9(b) illustrates the change of element segregation coefficient with treatment time at the melt treatment temperatures of 1,550 °C and 1,600 °C. As treatment time and temperature increase, the segregation coefficient of each element progressively gets closer to 1, although the pace of this convergence slows down over extended periods. This suggests that prolonging treatment time aids in achieving a uniform element distribution, consequently leading to a more homogeneous melt structure. However, the impact of this process diminishes over time. The segregation coefficient of the W element is considerably influenced by temperature, whereas those of Nb and Ti elements are predominantly affected by treatment time.

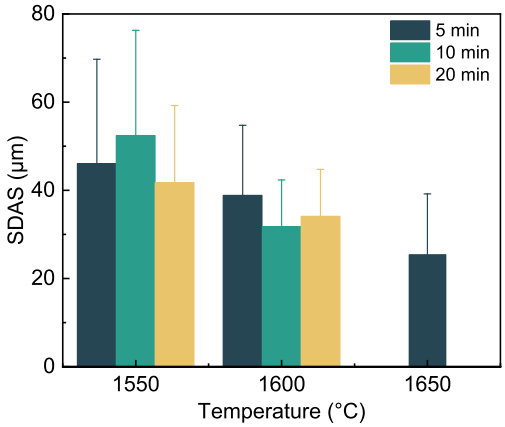

Fig. 8: SDAS of K424 superalloy superheated at different melt treatment conditions

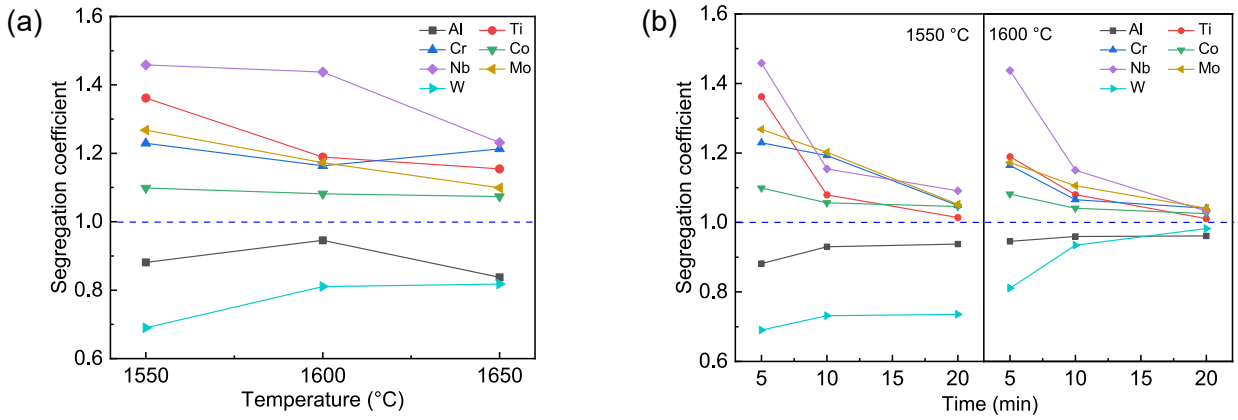

Fig. 9: Segregation coefficient of elements in K424 superalloy superheated at different conditions: (a) at temperatures of 1,550 °C, 1,600 °C, and 1,650 °C for a duration of 5 min; (b) at temperatures of 1,550 °C and 1,600 °C for a duration of 5, 10, and 20 min, respectively

3.5 Mechanical properties

Figure 10 shows the mechanical properties of K424 superalloy at varying melt treatment conditions, assessed at room temperature. An analysis of Figs. 10(a) to (c) reveals that all mechanical properties initially increase and then decrease with extended melt treatment time across different temperatures. At a treatment temperature of 1,550 °C, the yield and tensile strengths reach their peak values of 760.5 MPa and 917.5 MPa, respectively, after a holding time of 10 min. Concurrently, the elongation and area reduction reach their maximum values of 13.5% and 20.5%, respectively. When the treatment temperature rises to 1,600 °C, both the yield and tensile strengths reach their maximum values also after a holding time of 10 min. The yield strength peaks at 795 MPa, while the tensile strength reaches a maximum of 960 MPa. After holding for 10 min, the elongation and area reduction are relatively higher, which are 13.5% and 19.25%, respectively. It can be seen from the standard deviation that the property stability after treated at 1,600 °C is better than that treated at 1,550 °C. At the highest treatment temperature of 1,650 °C, the yield and tensile strengths reach their overall maximum values of 852.5 MPa and 1,007.5 MPa, respectively, after holding for 5 min. However, the standard deviation of yield strength is also the largest, indicating a compromised strength stability. The elongation and area reduction are lower at this temperature.

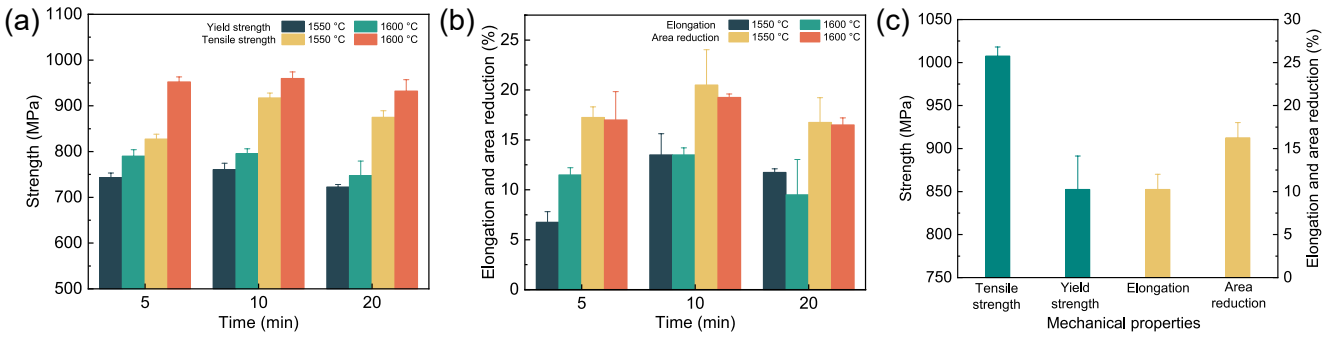

Fig. 10: Mechanical properties of K424 superalloy at 1,550 °C and 1,600 °C for a duration of 5, 10, and 20 min (a)–(b), and at 1,650 °C for a duration of 5 min (c)

In conclusion, the mechanical properties of the alloy at different treatment conditions exhibit a mix of strengths and weaknesses. Choosing the right treatment conditions requires a careful balance between the significance and stability of each property index, tailored to meet the specific demands of the intended application. For instance, a treatment at 1,650 °C for 5 min may be chosen for high strength, whereas a treatment at 1,600 °C for 10 min may be preferable for superior overall performance and stability.

Figure 11 depicts the stress rupture life of the K424 superalloy subjected to various melt treatments, tested under conditions of 975 °C and 196 MPa. Firstly, the melt treatment temperature significantly affects the stress rupture life of the K424 superalloy. With a treatment duration of 5 min, the stress rupture life substantially increases as the melt treatment temperature rises. When the treatment temperature is raised from 1,550 °C to 1,600 °C, the stress rupture life increases from 37.30 h to 44.11 h, and further increasing the temperature to 1,650 °C boosts the stress rupture life to 51.40 h. This indicates that within this temperature range, the durability of alloy is enhanced. Secondly, the melt treatment time also exerts a certain effect on the stress rupture life. The stress rupture life initially increases and then decreases with the extension of the melt treatment time. Taking the treatment temperature of 1,550 °C as an example, as the melt treatment time increases from 5 to 10 min, the stress rupture life slightly increases from 37.30 h to 37.64 h. However, when the melt treatment time extends to 20 min, the stress rupture life reduces to 35.09 h. This suggests that excessively long melt treatment time may lead to the degradation of material's properties. This trend is more pronounced at the treatment temperature of 1,600 °C. Furthermore, when treated at 1,550 °C and 1,600 °C, as the melt treatment time is extended from 5 min to 20 min, the standard deviation of stress rupture life shows an overall decreasing trend. Therefore, considering the standard deviation level of stress rupture life, extending the melt treatment time appears to be beneficial for enhancing the stability of durability.

In conclusion, the melt treatment temperature and the holding time are crucial factors influencing the stress rupture life of the K424 superalloy when tested under conditions of 975 °C and 196 MPa. Appropriate melt treatment temperatures and

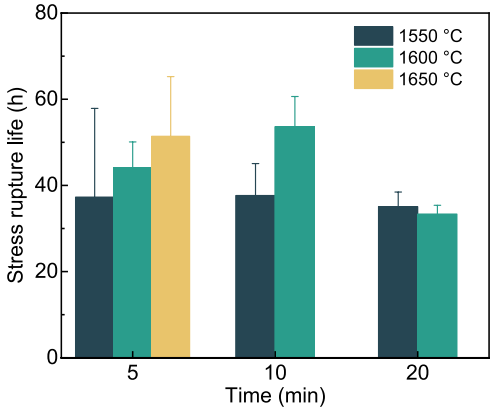

Fig. 11: Rupture life of K424 superalloy superheated at different melt superheating conditions

holding times can improve the stress rupture life of superalloy. Additionally, the standard deviation of the data indicates that the effect of treatment conditions on the consistency of stress rupture life is also an important consideration. Therefore, when optimizing the melt treatment process for K424 superalloy, both the stress rupture life and its consistency should be taken into account to ensure the reliability and stability of material performance.

4 Discussion

4.1 Influence of melt superheating on solidification characteristics and microstructures of K424 superalloy

Figure 12(a) reveals the solidification characteristic parameters of the alloy at various melt treatment conditions, thereby determining the nucleation undercooling and solidification range for the respective melt treatment scenarios. Figure 12(b) reveals that as the melt superheating temperature rises from 1,450 °C to 1,600 °C, the nucleation undercooling of the melt escalates from 5.28 °C to 23.72 °C, while the solidification range narrows from 9.02 °C to 6.08 °C. Notably, the nucleation undercooling exhibits a modest increase between 1,450 °C and 1,500 °C, but it surges markedly from 1,500 °C to 1,600 °C. The sudden increase or decrease in the level of undercooling indirectly reflects the changes in the cluster structure within the alloy melt [3]. These structural changes significantly affect the solidification characteristics, providing an essential basis for adjusting the microstructure and properties of the melt. Many researchers [8, 13, 14, 17] have investigated the structure of superalloy melts, their characteristics, and solidification behavior in relation to superheating temperature. The existence of two distinct anomalous temperatures, i.e., the first critical temperature (Tan1) and the second critical temperature (Tan2), marks the transitions in the structure of superalloy melts. Close to the liquidus temperature, nickel-based superalloy melts exhibit $Ni_3(Al, Ta)$ type cluster structures, along with refractory particles such as carbides and nitrides. Upon heating to the critical temperature Tan1, the medium-range ordered $Ni_3(Al, Ta)$ clusters undergo a transition to short-range ordered structures. Concurrently, refractory particles with sizes ranging from 1 to 10 nm dissolve and form new multicomponent clusters, resembling $Ni_3(Al, Ta)$ type clusters. As the temperature of melts approaches Tan2, these multicomponent cluster structures disintegrate, leading to a more homogenous melt structure and composition. For the K424 superalloy in this study, Tan1 could be determined to be about 1,500 °C, while Tan2 could be confirmed to be above 1,600 °C [Fig. 12(b)]. This signifies a substantial change in the melt structure of K424 superalloy at temperatures exceeding 1,500 °C, highlighting the crucial role of superheating the alloy within this specific temperature range.

The effect of melt treatment temperature on grain size can be explained by the classical nucleation theory. According to the classical nucleation theory, the critical nucleation size and the corresponding critical nucleation energy and nucleation rate can be expressed as follows [18]:

$$r^* = \frac{2\sigma T_m}{\Delta H_V \Delta T} \tag{1}$$

$$\Delta G^* = \frac{16\pi\sigma^3 T_m^2}{3\Delta H_V^2 \Delta T^2} \tag{2}$$

$$I = K \cdot e^{-\Delta G^*/kT} \cdot e^{-Q/kT} \tag{3}$$

where r^* is the critical nucleation radius, m; σ is the liquid-solid interface energy per unit area, $J \cdot m^{-2}$; T_m is the melting temperature of metal, K; ΔH_V is the melting enthalpy per unit volume of melt, $J \cdot m^{-3}$; ΔT is nucleation undercooling, K; ΔG^* is the critical nucleation work, $J \cdot m^{-3}$; K is the proportional constant, $s^{-1} \cdot m^{-3}$; I is the nucleation rate, $s^{-1} \cdot m^{-3}$; k is Boltzmann constant; T is nucleation temperature, K; and Q is the diffusion activation energy of metal atoms through the solid-liquid interface, $J \cdot m^{-3}$.

Equations (1) through (3) demonstrate that an increase in nucleation undercooling reduces the critical nucleation radius and energy, thereby enhancing the nucleation rate and eventually leading to an increase in the number of grains. Within a given solidification region, the more grain number results in a reduction of individual grain size, contributing to a grain refinement effect.

Secondary dendritic arm spacing is a significant parameter that characterizes the solidification structure. According to

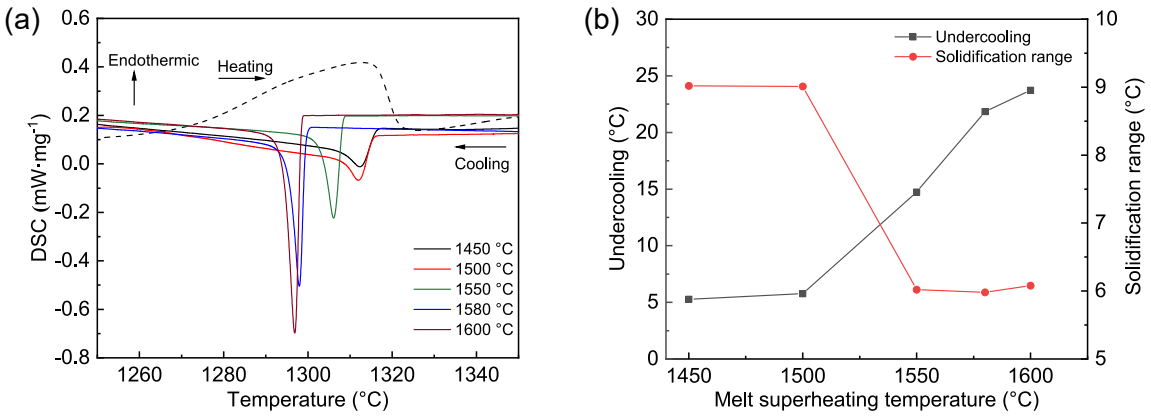

Fig. 12: (a) DSC curves at various melt treatment temperatures; (b) undercooling and solidification range based on the DSC findings

the Kurz-Fisher model, secondary dendrite arm spacing (λ_2) is correlated with the non-equilibrium solidification temperature range, as described by the following equation [19]:

$$\lambda_2 = 5.5\left(M\frac{\Delta T'}{\dot{T}}\right)^{1/3} \quad (4)$$

where M is a coefficient related to the alloy composition, which varies minimally and is typically regarded as a constant; $\Delta T'$ is the non-equilibrium solidification range, K; $\dot{T}$ is the cooling rate, K·s^{-1}. In this research, the raw materials originate from a single batch, and the cooling rate for each experimental group is uniformly maintained, therefore, $\dot{T}$ can be allowed to treat as invariable constants. Consequently, it can be concluded from Eq. (4) the secondary dendrite arm spacing λ_2 decreases as $\Delta T'$ decreases. The study reveals that as the melt treatment temperature increases, the solidification range decreases, as depicted in Fig. 12(b). This trend explains the observed variations in the size of the secondary dendrites illustrated in Fig. 8.

It is important to recognize that the duration of melt treatment also influences the alteration of the melt structure. The transformation of certain cluster structures and the breakdown of particles within the melt necessitate a specific duration of holding time, which is calculated as follows [20]:

$$t\big|_{r\to 0} = \frac{1}{16\pi^3 D\beta}\left[\frac{\sigma(1+\beta)}{L(1+k)}\right]^2 k_T^3 \quad (5)$$

where t is the holding time required for melt treatment, s; r is the radius of the unmelted particles in the melt, m; D is the diffusion coefficient of particles in the melt, m^2·s^{-1}; σ is the surface energy, J·m^{-2}; β is the dimensionless structure coefficient ($\beta=L_M/CT_0$, where L_M is the atomic heat of crystallization, J·mol^{-1}; C is the atomic heat capacity of the melt, J·K^{-1}·mol^{-1}; T_0 is the overheating temperature, K); k_T is the temperature criterion, $k_T=T_0/\Delta T$ (where ΔT is the undercooling, K); k is a dimensionless coefficient, $k=k_T/\beta$; L is the product of S_m by T_0 (S_m is the entropy of melting, J·m^{-3}·K^{-1}).

According to Eq. (5), the dissolution time of unmelted particles within the melt correlates with the surface tension, diffusion coefficient, supercooling degree, and additional physical parameters, all of which are intricately linked to the chemical composition of melt. If the melt treatment duration exceeds the time necessary for the unmelted particles to dissolve, these particles can be essentially fully dissolved in the melt.

4.2 Influence of melt superheating on solute partition coefficient of K424 superalloy

The variation in elemental segregation in K424 nickel-based superalloy is predominantly attributed to the melt superheating treatment. This process results in modifications in the melt structure, affects the arrangement of atoms within the melt, and consequently leads to changes in the distribution of solute elements within melt prior to solidification. Moreover, the melt treatment enhances the diffusion of elements within the solidified alloy, and the diffusion coefficient can be determined by the Arrhenius equation [21]:

$$D = D_0 e^{-Q/k_B T} \quad (6)$$

where D_0 is the pre-exponential factor, m^2·s^{-1}; Q is activation energy, J; k_B is the Boltzmann constant, J·K^{-1}; and T is the absolute temperature, K.

DSC results in Fig. 12(a) reveal that an increase in melt treatment temperature causes a leftward shift in the curve, signifying a decrease in the nucleation temperature of the K424 alloy. Extending the melt treatment duration appropriately enhances the homogenization of the melt composition without depleting elemental content, consequently increasing undercooling and further lowering the nucleation temperature. Fredriksson et al. [7] suggests a liner relationship between the activation energy and the nucleation temperature of an alloy: A reduction in the nucleation temperature means a concomitant decrease in activation energy. As assumed in Eq. (6), a diminished activation energy results in an augmented diffusion coefficient of atoms, which in turn improves their diffusion rate within the solid phase matrix and mitigates elemental segregation. Therefore, optimal melt treatment conditions, in terms of both temperature and duration, are crucial for achieving a homogenized melt structure. They also play a vital role in facilitating elemental diffusion in the solidified alloy, thereby reducing the potential for elemental segregation.

4.3 Influence of melt superheating on mechanical properties of K424 superalloy

Tensile properties at room temperature and stress rupture life are crucial parameters for assessing whether K424 superalloy satisfies usage requirements. The influence of grain size on the mechanical characteristics of alloys has been a subject of interest for decades. In the 1950s, Hall and Petch introduced the Hall-Petch relationship, derived from their studies on low-carbon steel [22, 23]:

$$\sigma = \sigma_0 + K_d d^{-1/2} \quad (7)$$

where σ is the yield strength of the metallic material; σ_0 is the frictional resistance of the grain against dislocation movement; K_d is the level of stress concentration at the grain boundary caused by dislocation accumulation, which correlates with the number of effective slip systems; d is the grain diameter. Equation (7) illustrates the quantitative correlation between grain size and yield strength. As the grain is refined, the yield strength of the material enhances, concurrently boosting the tensile strength, as depicted in Figs. 6 and 10. However, this study reveals that while the strength of the alloy is enhanced, the corresponding plasticity diminishes to various extents.

Nevertheless, Eq. (7) does not pertain to the deformation behavior of polycrystalline alloys across all temperature ranges. The influence of grain size on the tensile strength of nickel-based polycrystalline alloys during creep varies between medium temperatures (700 °C to 900 °C) and high temperatures (above 900 °C) [4]. The study of Du et al. [24] demonstrates that at 760 °C, cracks propagate transgranularly. At this temperature,

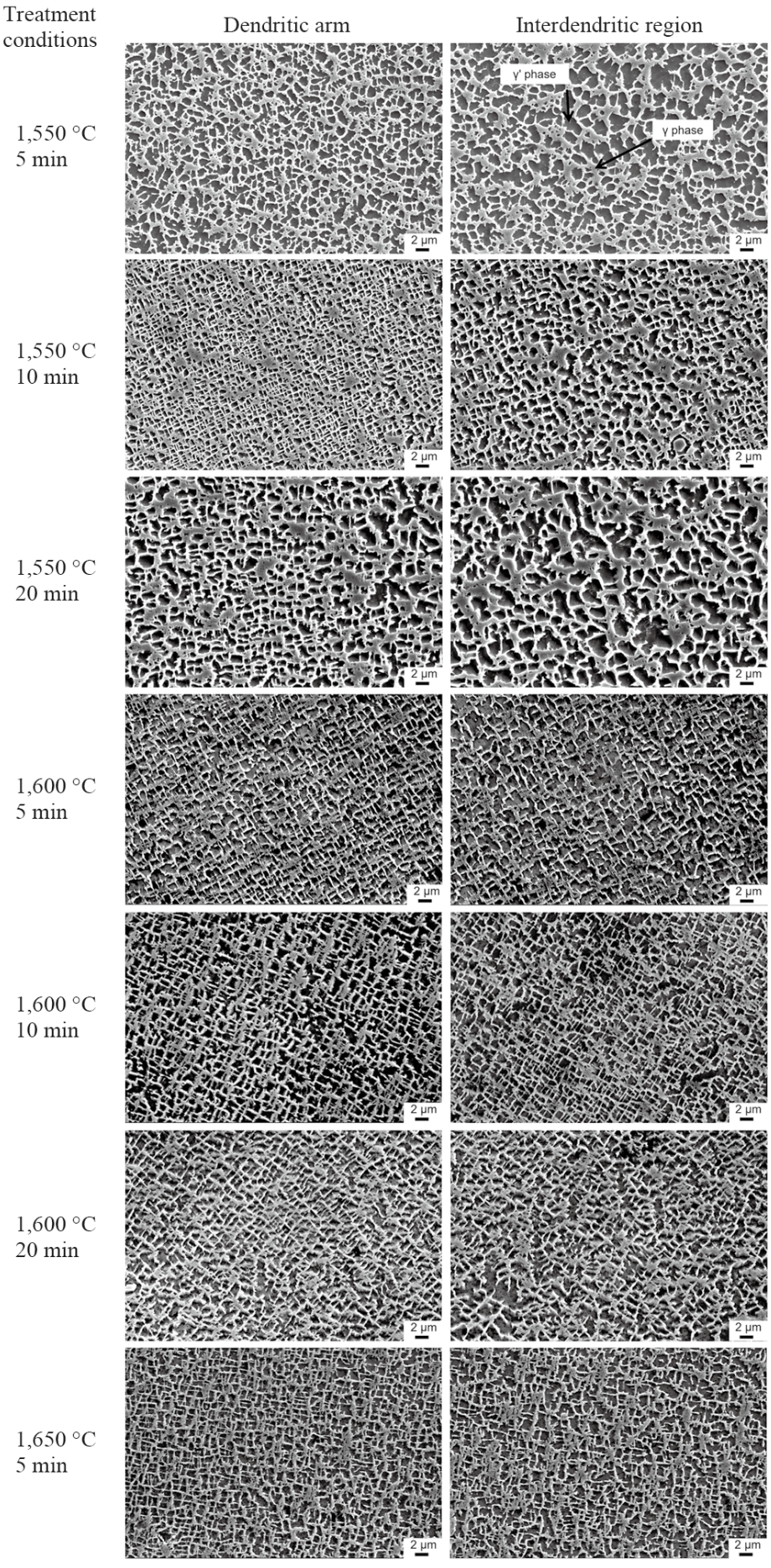

Fig. 13: As-cast morphologies of γ' phase at different melt superheating conditions

the grain boundary strength surpasses the intragranular strength, leading to plastic deformation primarily through intragranular slip system activation. Consequently, a smaller grain size results in shorter slip band lengths, more uniform deformation within grains, easier coordinated deformation among grains, and enhanced creep resistance [25]. In contrast, at 950 °C during creep, cracks exhibit an intergranular fracture pattern, with plastic deformation localized at the grain boundaries, indicative of a pronounced grain boundary slip mode [4]. Even beyond 900 °C, the stress rupture life of the K424 superalloy is prolonged as the grain size diminishes, suggesting that grain size is not the sole determinant of stress rupture life. The improvement of element segregation may be one of the factors to improve the stress rupture life. The uniform distribution of atoms in the matrix may improve the properties of grain boundary carbides, subsequently strengthen the grain boundary and ultimately improving the stress rupture life. However, this hypothesis requires further investigation and research to validate.

Moreover, the size of the γ' phase in nickel-based superalloys is crucial for augmenting their high-temperature mechanical performance [26]. Reducing the γ' phase size and increasing its content not only significantly improves the yield strength of nickel-based superalloys [27-29], but also extends their creep rupture life [30-32]. Figure 13 illustrates the morphological characteristics of the γ' phase in the K424 as-cast structure under varying melt treatment conditions. In general, the trend exhibited by the size of the γ' phase with respect to melt treatment temperature and duration aligns with the trends observed in grain size under similar conditions. This correlation can be ascribed to the influence of melt treatment on the nucleation and growth processes of the γ' phase. The melt treatment affects the size of the γ' phase, and the variations in its size significantly affects the mechanical properties of the alloy [27, 33, 34]. Additionally, Fig. 13 reveals that the γ' phase within the interdendritic regions is typically larger than that within the dendrite. This discrepancy is due to higher supersaturation levels in the interdendritic regions during the solidification of alloy melt, promoting preferential nucleation of the γ' phase in these areas [35]. Consequently, the γ' phase in the interdendritic regions has more space to grow, resulting in larger sizes. These findings are in agreement with those reported in Ref. [36]. Furthermore, as the melt treatment temperature rises, the size disparity of the γ' phase between dendrites and interdendritic regions diminishes. This indicates that melt treatment enhances the elemental distribution within the melt. Such treatment not only influences grain nucleation but also the nucleation of the γ' phase, thereby improving the alloy's mechanical properties through microstructural refinement and homogenization.

5 Conclusions

The impact of melt superheating temperature on the nucleation undercooling of K424 superalloy was examined through DSC analysis. The influence of superheating temperature and its duration on the alloy's solidification structure and mechanical properties was further explored through casting experiments. The effects of various melt treatment conditions on grain size, secondary dendrite arm spacing, elemental segregation, and mechanical properties were also analyzed. The main findings are summarized as follows:

(1) The temperature of the melt superheat treatment exerts a significant impact on the characteristic temperature of the K424 superalloy. As the melt superheating temperature increases from 1,450 °C to 1,600 °C, the nucleation undercooling of the melt correspondingly rises from 5.28 °C to 23.72 °C.

(2) The grain size in the as-cast solidification structure of K424 superalloy can be effectively controlled by adjusting the melt superheating time and temperature. It has been demonstrated that the smallest average grain size of 949 μm can be achieved with a melt superheating treatment at 1,650 °C for 5 min.

(3) The influence of the melt treatment temperature on SDAS is markedly more significant than that of the treatment duration. The smallest recorded SDAS, measuring 25.38 μm, is detected when the superalloy is subjected to a melt treated at 1,650 °C for a duration of 5 min.

(4) The segregation of Al and W elements occurs in the dendrite arm, while Ti, Cr, Co, Nb, and Mo elements are segregated in the interdendrite region. With the increase of melt treatment time, the segregation coefficient of each element gradually tends to 1, but the rate of convergence slows down. At a melt treatment temperature of 1,650 °C, the segregation coefficients for Al and Cr elements rise, potentially owing to alterations in the melt structure and the consumption of these elements at elevated superheat temperatures.

(5) The mechanical properties and stress rupture life of K424 superalloy are significantly influenced by melt treatment temperature and holding time. Optimal mechanical strength is achieved at 1,650 °C with a short holding time of 5 min, while a balance of strength and stability is found at 1,600 °C with a holding time of 10 min. The stress rupture life increases with temperature up to 1,650 °C with a holding time of 5 min. However, both strength and stress rupture life can degrade with an excessive holding time. Consistency in properties, as indicated by standard deviations, also varies with treatment conditions, highlighting the need for careful selection of temperature and time to balance performance and reliability.

Acknowledgments

This research was financially supported by the Natural Science Foundation Joint Fund of Liaoning Province, China (No. 2023-MSLH-342).

Conflict of interest

The authors declare that they have no known competing financial interests or personal relationships that could have appeared to influence the work reported in this paper.

References

[1] Donachie M J, Donachie S J. Superalloys: A technical guide, 2nd Ed., Ohio. ASM International, 2002: 79–90.
[2] Pollock T M, Tin S. Nickel-based superalloys for advanced turbine engines: Chemistry, microstructure and properties. Journal of Propulsion and Power, 2006, 22(2): 361–374.
[3] Zhang J, Jie Z Q, Huang T W, et al. Research and development of equiaxed grain solidification and forming technology for nickel-based cast superalloys. Acta Metallurgica Sinica, 2019, 55(9): 1145–1159.
[4] Zhang C J, Wang P, Wen Z X, et al. Study on creep properties of nickel-based superalloy blades based on microstructure characteristics. Journal of Alloys and Compounds, 2021, 890.
[5] Wu Y T, Li C, Li Y F, et al. Effects of heat treatment on the microstructure and mechanical properties of Ni_3Al-based superalloys: A review. International Journal of Minerals, Metallurgy and Materials, 2021, 28(4): 553–566.
[6] Qiu C L, Wu X H, Mei J F, et al. Influence of heat treatment on microstructure and tensile behavior of a hot isostatically pressed nickel-based superalloy. Journal of Alloys and Compounds, 2013, 578: 454–464.
[7] Fredriksson H, Fredriksson E. A model of liquid metals and its relation to the solidification process. Materials Science and Engineering: A, 2005, 413–414: 455–459.
[8] Yin F S, Sun X F, Guan H R, et al. Effect of thermal history on the liquid structure of a cast nickel-base superalloy M963. Journal of Alloys and Compounds, 2004, 364(1–2): 225–228.
[9] Calvo-Dahlborg M, Popel P S, Kramer M J, et al. Superheat-dependent microstructure of molten Al-Si alloys of different compositions studied by small angle neutron scattering. Journal of Alloys and Compounds, 2013, 550: 9–22.
[10] Wang L N, Sun X F, Guan H R. Effect of melt heat treatment on MC carbide formation in nickel-based superalloy K465. Results in Physics, 2017, 7: 2111–2117.
[11] Bodakin N E, Baum B A, Kostina T K. Effect of melting conditions on the thermal expansion coefficient of alloy 36N. Metal Science and Heat Treatment, 1979, 21: 323–325.
[12] Su H J, Wang H F, Zhang J, et al. Influence of melt superheating treatment on solidification characteristics and rupture life of a third-generation Ni-based single-crystal superalloy. Metallurgical and Materials Transactions: B, 2018, 49(4): 1537–1546.
[13] Kolotukhin E V, Tjagunov G V. Crystallization of superalloys with various contents of carbon. Journal of Materials Processing Technology, 1995, 53: 219–227.
[14] Tyagunov A G, Baryshev E E, Kostina T K, et al. Thermal stability of the structure of a high-temperature nickel alloy fabricated by two different technologies. Metal Science and Heat Treatment, 1999, 41: 538–541.
[15] Jie Z Q, Zhang J, Huang T W, et al. The influence of melt superheating treatment on the cast structure and stress rupture property of IN718C superalloy. Journal of Alloys and Compounds, 2017, 706: 76–81.
[16] Academic Committee of the Superalloys, CSM, China Superalloys Handbook. Beijing: Standards Press of China, 2012: 168–176. (In Chinese)
[17] Kurakova N V, Molokanov V V, Sterkhova I V, et al. Effect of the state of a melt on the glass-forming ability, structure, and properties of a melt-quenched bulk amorphous nickel-based alloy. Russian Metallurgy (Metally), 2007, 6: 519–523.
[18] Zhai Q J. Foundamentals of structure refinement technology for metal solidification. Beijing: Science Press, 2018: 26–27. (In Chinese)
[19] Kurz W, Fisher D J. Fundamentals of solidification. Switzerland: Trans. Tech. Publication, 1998: 88–96.
[20] Balakin Y A, Gladkov M I. Thermodynamic analysis of high-temperature treatment of metallic melts: Part II. Russian Metallurgy (Metally), 2008, 8: 730–733.
[21] Koju R K, Mishin Y. Atomistic study of grain-boundary segregation and grain-boundary diffusion in Al-Mg alloys. Acta Materialia, 2020, 201: 596–603.
[22] Hall E O. The deformation and ageing of mild steel. Proceedings of the Physical Society, 1951, B64: 747–753.
[23] Petch N J. The cleavage strength of polycrystals. Journal of the Iron and Steel Institute, 1953, 174: 25.
[24] Du B N, Yang J, X, Cui C Y, et al. Effects of grain refinement on creep properties of K417G superalloy. Acta Metallurgica Sinica, 2014, 50(11): 1384–1392.
[25] Soula A, Renollet Y, Boivin D, et al. Analysis of high-temperature creep deformation in a polycrystalline nickel-base superalloy. Materials Science and Engineering: A, 2009, 510–511: 301–306.
[26] Everitt S, Starink M J, Pang H T, et al. A comparison of high temperature fatigue crack propagation in various subsolvus heat treated turbine disc alloys. Materials Science and Technology, 2007, 23(12): 1419–1423.
[27] Wang W Z, Hong H U, Kim I S, et al. Influence of γ′ and grain boundary carbide on tensile fracture behaviors of Nimonic 263. Materials Science and Engineering: A, 2009, 523(1–2): 242–245.
[28] Ceena J, Christer P M H C. Influence of heat treatment on the microstructure and tensile properties of Ni-base superalloy Haynes 282. Materials Science and Engineering: A, 2017, 679: 520–530.
[29] Shin K Y, Kim J H, Mathieu T, et al. Effects of heat treatment on the microstructure evolution and the high-temperature tensile properties of Haynes 282 superalloy. Materials Science and Engineering: A, 2019, 751: 311–322.
[30] Nathal M V. Effect of initial gamma prime size on the elevated temperature creep properties of single crystal nickel base superalloys. Metallurgical Transactions: A, 1987, 18(11): 1961–1970.
[31] Mazur Z, Luna-Ramírez A, Juárez-Islas J A, et al. Failure analysis of a gas turbine blade made of Inconel 738LC alloy. Engineering Failure Analysis, 2005, 12(3): 474–486.
[32] Peng Z C, Tian G F, Jiang J, et al. Mechanistic behaviour and modelling of creep in powder metallurgy FGH96 nickel superalloy. Materials Science and Engineering: A, 2016, 676: 441–449.
[33] Gayda J, Miner R V. The effect of microstructure on 650 °C fatigue crack growth in P/M astroloy. Metallurgical Transactions: A, 1983, 14(11): 2301–2308.
[34] Pang H T, Reed P A S. Microstructure variation effects on room temperature fatigue threshold and crack propagation in Udimet 720Li Ni-base superalloy. Fatigue & Fracture of Engineering Materials & Structures, 2009, 32(8): 685–701.
[35] Xiao J M. Alloy phase and phase transformation. Beijing: Metallurgical Industry Press, 1987. (In Chinese)
[36] Cui H Y, Tan Y, Bai R S, et al. Effect of melt superheat treatment on solidification behavior and microstructure of new Ni-Co based superalloy. Journal of Materials Research and Technology, 2021, 15: 4970–4980.